Simulations of Processes Associated with the Fast Warming Rate of the Southern Midlatitude Ocean

WENJU CAI AND TIM COWAN

Wealth from Oceans National Research Flagship, CSIRO, Aspendale, Victoria, Australia

STUART GODFREY AND SUSAN WIJFFELS

Wealth from Oceans National Research Flagship, CSIRO, Hobart, Tasmania, Australia

(Manuscript received 6 February 2009, in final form 20 July 2009)

ABSTRACT

Significant warming has occurred across many of the world's oceans throughout the latter part of the twentieth-century. The increase in the oceanic heat content displays a considerable spatial difference, with a maximum in the 35°–50°S midlatitude band. The relative importance of wind and surface heat flux changes in driving the warming pattern is the subject of much debate. Using wind, oceanic temperature, and heat flux outputs from twentieth-century multimodel experiments, conducted for the Fourth Assessment Report (AR4) of the Intergovernmental Panel on Climate Change (IPCC), the authors were able to reproduce the fast, deep warming in the midlatitude band; however, this warming is unable to be accounted for by local heat flux changes. The associated vertical structure and zonal distribution are consistent with a Sverdrup-type response to poleward-strengthening winds, with a poleward shift of the Southern Hemisphere (SH) supergyre and the Antarctic Circumpolar Current. However, the shift is not adiabatic and involves a net oceanic heat content increase over the SH, which can only be forced by changes in the net surface heat flux. Counterintuitively, the heat required for the fast, deep warming is largely derived from the surface heat fluxes south of 50°S, where the surface flux into the ocean is far larger than that of the midlatitude band. The heat south of 50°S is advected northward by an enhanced northward Ekman transport induced by the poleward-strengthening winds and penetrates northward and downward along the outcropping isopycnals to a depth of over 1000 m. However, because none of the models resolve eddies and given that eddy fluxes could offset the increase in the northward Ekman transport, the heat source for the fast, deep warming in the midlatitude band could be rather different in the real world.

1. Introduction

An interesting feature of future sea level projection is a band of pronounced sea level rise stretching across the midlatitude southern Atlantic, Indian, and Pacific Oceans [see Fig. 10.32 in chapter 10 of Meehl et al. (2007)]. One may expect a similar pattern in ocean heat content trends over the past decades, given the substantial warming that has already occurred (e.g., Levitus et al. 2000, 2005; Barnett et al. 2005; Delworth et al. 2005; Pierce et al. 2006). Such an indication is seen in the altimetric and thermosteric patterns of sea level change over the 1993–2003 period; however, the trend pattern over a longer period is less clear, mainly because of limited available measurements. Using historic shipboard measurements collected since 1930 and Autonomous Lagrangian Circulation Explorer float measurements collected during the 1990s, Gille (2002) showed that the warming rate of the Southern Ocean in the 700- to 1100-m depth is indeed twice as fast as the upper 1000 m of the World Ocean as a whole (Levitus et al. 2000), providing the evidence for such latitudinal differentiation over the longer period. Palmer et al. (2007) identified a warming trend of 0.12 W m^{-2} in waters warmer than 14°C, using millions of oceanic profiles collected from 1961 to 2003. Newly compiled ocean temperature trends by Wijffels et al. (2008), using observations compiled from 1960 to 2007 and after correcting for instrumental errors, further confirm the fast warming rate over the upper 2000 m of the midlatitude Southern Ocean (Fig. 1).

Corresponding author address: Wenju Cai, CSIRO Marine and Atmospheric Research, PMB 1, Aspendale, VIC 3195, Australia.
E-mail: wenju.cai@csiro.au

DOI: 10.1175/2009JCLI3081.1

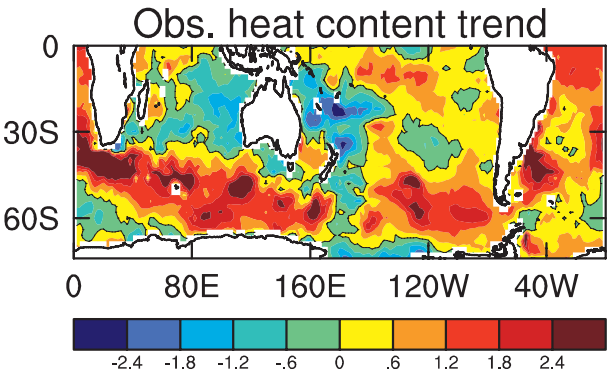

FIG. 1. Observed total trend in the upper 2000-m oceanic heat content ($\times 10^9$ J m^{-2} per 48 years) over 1960–2007 after correcting for instrumental errors (Wijffels et al. 2008).

The consensus is that the warming is likely due to anthropogenic forcing (Gille 2002; Banks and Wood 2002; Hansen et al. 2005; Gille 2008) and that it is somewhat mitigated by a volcanic forcing (Fyfe 2006; Church et al. 2005) and anthropogenic aerosols (Cai et al. 2006; Cai and Cowan 2007a). However, vigorous debate persists regarding the relative importance of wind and surface heat flux forcing. Pierce et al. (2006) illustrate that the warming is unable to be explained by a local vertical heat balance. Barnett et al. (2005) find substantially larger net surface heat fluxes into the Southern Hemisphere (SH) ocean than the Northern Hemisphere (NH) ocean. Hansen et al. (2005) suggest that an even larger flux of 0.86 ± 0.12 W m^{-2} has gone into the SH oceans during the last decade, supporting the recent acceleration of ocean warming.

The ''wind-driven'' hypothesis focuses on a more regional scale and emphasizes the role of near-''adiabatic'' processes, including a southward shift in the circumpolar front (Suzuki et al. 2005), a subduction of warm anomalies in the region of the subantarctic mode water formation (Banks and Wood 2002), and both a poleward shift in the midlatitude gyre circulation (Cai et al. 2005; Cai 2006; Alory et al. 2007) and the Antarctic Circumpolar Current (ACC; Gille 2008). These changes are attributable to anthropogenic climate change as a consequence of a consistent poleward shift in the westerly winds (Cai et al. 2005; Yin 2005) associated with an upward trend of the southern annular mode (SAM) over the past few decades, driven by increases in greenhouse gases and stratospheric ozone depletion (Thompson and Solomon 2002; Arblaster and Meehl 2006; Cai and Cowan 2007b). However, a long-term trend, inferred from the newly available Argo float data referenced to the subsurface ocean syntheses in the World Ocean Atlas Series, indicates both a downward and southward displacement of isopycnals (Roemmich and Gilson 2009), suggesting that wind forcing alone does not represent the full picture. Because of limited measurements and the lack of heat flux observations, their relative importance in the observed trend may never be known.

Several investigations have turned to ocean-only and/or fully coupled climate models to evaluate the role of wind. However, there is no ''clean'' way of isolating the impacts of wind and surface air–sea heat flux components. Fyfe et al. (2007) forced a coupled model both with and without the Intergovernmental Panel on Climate Change Fourth Assessment Report (IPCC AR4) ensemble-averaged wind changes (with poleward-intensifying winds), in conjunction with and without an observed CO_2 increase to quantify the wind effect. The wind-only experiment shows that the wind change is key in determining its latitudinal structure, but it is unclear whether the heat is conserved in such an experiment because many flux fields respond to such wind changes. In an ocean-only framework (e.g., Oke and England 2004), wind forcing is usually applied in conjunction with a restoration condition on temperature to keep the model in check; an imposed wind change always induces alterations to the implied heat flux. Imposing an observed wind trend in a coupled environment will generate changes in surface heat fluxes because turbulent heat fluxes respond to wind and wind-induced changes in sea surface temperature (SST). Further, there are no long-term observations of net heat fluxes for an assessment of its impact. The latest series of twentieth-century experiments, performed as part of the Third Coupled Model Intercomparison Project (CMIP3) in support of the IPCC AR4, provides an opportunity to explore the role of wind and heat fluxes because wind data and the components of heat flux are available to allow a heat budget analysis.

2. Data and model experiments

We use outputs from one simulation of the late twentieth-century climate from 17 CMIP3 models. It is worth noting that none of the CMIP3 models resolve eddies. All of the models incorporate forcing from anthropogenic aerosols and increasing CO_2, but only 10 models include volcanic aerosols. We choose these models because of the availability of outputs of heat fluxes and oceanic temperature, as well as the corresponding preindustrial control runs required to correct the drift that exists in many climate models. Monthly anomalies of full-depth temperature, wind, and surface heat fluxes are constructed for the 1951–99 period by removing the 49-year climatological mean. Trends are also calculated over this same period. Heat fluxes and

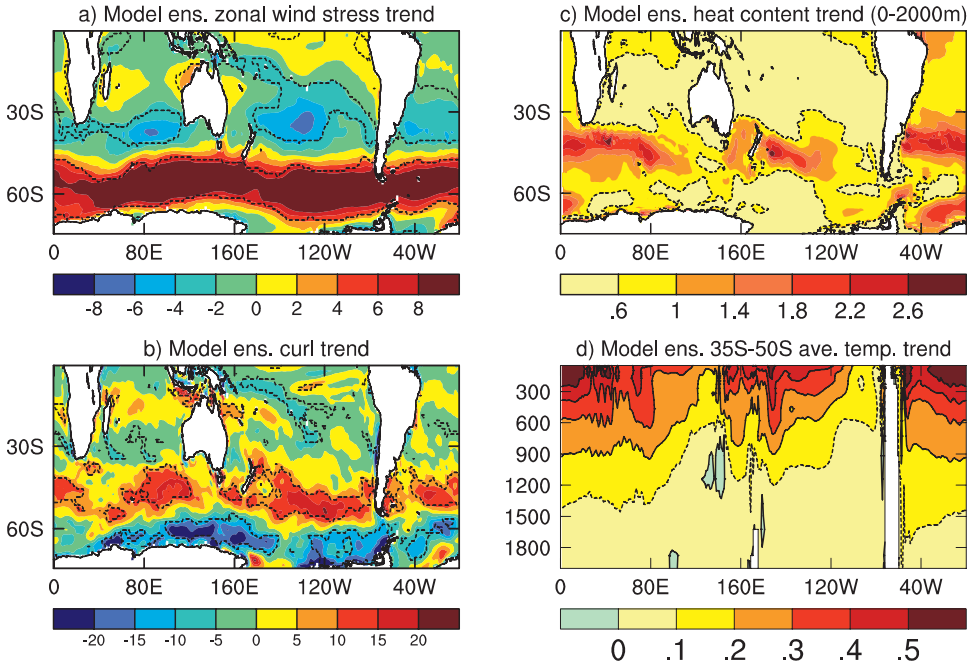

FIG. 2. All-model ensemble-mean total trends for 1951–99 in (a) zonal wind stress ($\times 10^{-3}$ N m^{-2} per 49 years), (b) wind stress curl ($\times 10^{-3}$ N m^{-3} per 49 years), (c) heat content over the upper 2000 m ($\times 10^{9}$ J m^{-2} per 49 years), and (d) the 35°–50°S latitudinal averaged temperature at all longitudes in the upper 2000 m (°C per 49 years). Significant trends at the 95% confidence level are shown as areas within the dashed lines.

oceanic heat content for the upper 2000 m and full depth are calculated for each model simulation, then interpolated onto a common grid and averaged to produce an ensemble mean. A comparable model ensemble climatology is also produced. Because CMIP3 climate models do not include a net heat flux output, such a field is constructed from latent and sensible heat fluxes, as well as the upwelling and downwelling components of longwave and shortwave radiation fluxes. Positive (negative) heat fluxes indicate ocean absorption (release) of heat at the ocean surface.

To compare the role of local heat fluxes in forcing the heat content trend in a latitude band, for a given surface heat flux change ($\overline{F_{\text{surf}}}$) averaged over 1951–99, the implied heat content trend (HC_{imp}) is inferred from the relationship

$$\text{HC}_{\text{imp}} = \overline{F_{\text{surf}}} AT,$$

where A is the total global ocean surface area and T is the total time over 1951–99 (in seconds). The actual total heat content trend (HC_{act}) is calculated as

$$\text{HC}_{\text{act}} = \int\int\int \rho C_p \Theta \, dV,$$

where ρ is the water density, C_p is the specific heat of seawater, Θ is the change in potential temperature, and V is the water volume. When compared with HC_{imp}, this gives a simple heat budget, indicating the role of horizontal heat transfer into and out of a given latitude band. The SH latitude bands of interest are where the ocean warming or surface heat fluxes are most prominent (50°–35°S and 90°–50°S).

In the following sections, we analyze the role of the wind forcing in the recent Southern Ocean warming (section 3), the associated poleward shift of the midlatitude gyres (section 4), and the extent to which SH heat fluxes feed into these large-scale oceanic changes (section 5).

3. Evidence for a wind-forcing case

a. Sverdrup-type responses

Trends of an all-model average zonal wind stress (Fig. 2a) and its curl (Fig. 2b) display familiar features (Cai and Cowan 2007b). First, there is a reduction in zonal wind stress in the midlatitudes and an increase in the higher latitudes. The latitudes of zero zonal wind change are located at around 45°S. Second, the all-model average trend of the wind stress curl, which is dominated

by the meridional gradient of zonal wind stress, displays maximum changes at approximately 45°–50°S. The climatological zero-curl line, which is located at 48.4°S in terms of a zonal average (not shown), extends across the three ocean sectors forming the ''supergyre'' (Cai 2006; Ridgway and Dunn 2007). This zero-curl line marks the separation point of the ACC from the gyre circulation. The positive curl change pushes the zero-curl line to 49.1°S (a 0.7° latitude southward shift) and signifies a poleward shift of the supergyre, as illustrated by forcing Godfrey's Island Rule model (Godfrey 1989) with similar wind changes (Cai 2006).

The meridional structure of temperature trends suggests that the Ekman convergence associated with the wind changes is important. Total trends of oceanic heat content (e.g., upper 2000 m, Fig. 2c) display a maximum warming along approximately 43°S, which is similar to the observed (Fig. 1). The location of maximum warming coincides with the latitude of the zero zonal wind change (Fig. 2a). To the north, westerlies decrease, generating a southward Ekman transport, whereas to the south westerlies intensify, inducing a northward Ekman transport. Thus, a strong Ekman convergence is formed at approximately 43°S. In the 50°–35°S midlatitude band, the full depth-integrated heat content shows an increasing trend of 6.46×10^{22} J, compared to a trend of 4.43×10^{22} J over a far larger area from 50°S to the Antarctic coast.

Wind changes impact the deep ocean, via Rossby wave adjustment, eventually leading to steady-state Sverdrup balance. The impact of the adjustment is conducted through an annular-scale integration of the wind stress curl changes from an eastern boundary to a western boundary, which are the two sides of the South American continent in this latitude band. The imprint of an east-to-west integration by Rossby waves manifests in the feature that the warming rate is slowest off the western side of South America (the eastern boundary of the South Pacific), where heat is distributed to a shallower depth but fastest and deepest off the eastern side of South America, or the western boundary of the South Atlantic (Fig. 2d). Thus, the location of Ekman convergence, its alignment with the southern midlatitude fast warming rate, and the zonal and vertical structure of the warming all imply a role by the wind changes.

b. *Pattern of wind-driven depth-integrated steric height*

If the coupled system is in a steady state, a Sverdrup-like wind-driven circulation model, such as Godfrey's Island Rule model (Godfrey 1989), may be used to predict where the ocean is storing the heat, regardless of where the heat is derived. A primary assumption of the Island Rule model is that the wind forcing has acted on the ocean for a time scale long enough so that a steady state is a good approximation. The Rossby wave time scale increases with latitude, and in the 35°–50°S midlatitude band considered here, a 49-year duration may not satisfy this condition. However, climate models predict that the SAM and the associated wind trends will persist and intensify as global warming continues (Fyfe et al. 1999; Kushner et al. 2001; Cai et al. 2003). Following such a scenario, while the wind and curl trends will not stabilize at values shown in Figs. 2a and 2b, the trend pattern may be similar. It is therefore instructive to examine how such wind changes, if stabilized, will distribute heat. To this end, we apply the Island Rule model to the wind changes to calculate wind-driven depth-integrated steric height (DISH), which is a measure of the integrated wind-driven energy stored in the ocean. The result is shown in Fig. 3. Temperature changes contribute to a significant portion of the DISH trend, such that the pattern of change coincides with the pattern of warming. We see that maximum DISH changes (Fig. 3, color) occur in the 35°–50°S midlatitude band, closely aligning with the model oceanic heat content pattern averaged over the upper 2000 m (Fig. 3, contours). Thus, wind changes will generate oceanic circulation trends that have the effect of storing heat in this midlatitude band, regardless of where the heat is derived.

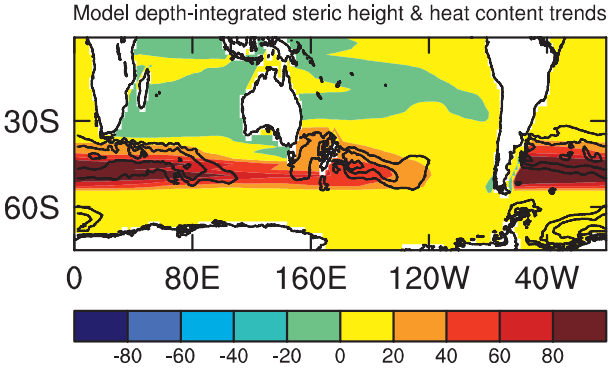

FIG. 3. Wind-driven depth-integrated steric height changes (contour; m^{-2}) obtained by applying the wind changes to Godfrey's Island Rule model. Superimposed is the all-model ensemble-mean total trend in heat content over the upper 2000 m [contours of 1.2, 1.8, and 2.4 ($\times 10^9$ J m^{-2} per 49 years) are plotted].

4. Poleward shift of the SH circulation

Several studies have suggested that the fast warming rate in the 35°–50°S midlatitude band could be explained by a poleward shift of the SH circulation including the ACC (Cai et al. 2005; Cai 2006; Alory et al. 2007; Gille 2008). This is consistent with the fact that the zero-curl line has shifted poleward by about 0.7° in latitude, as

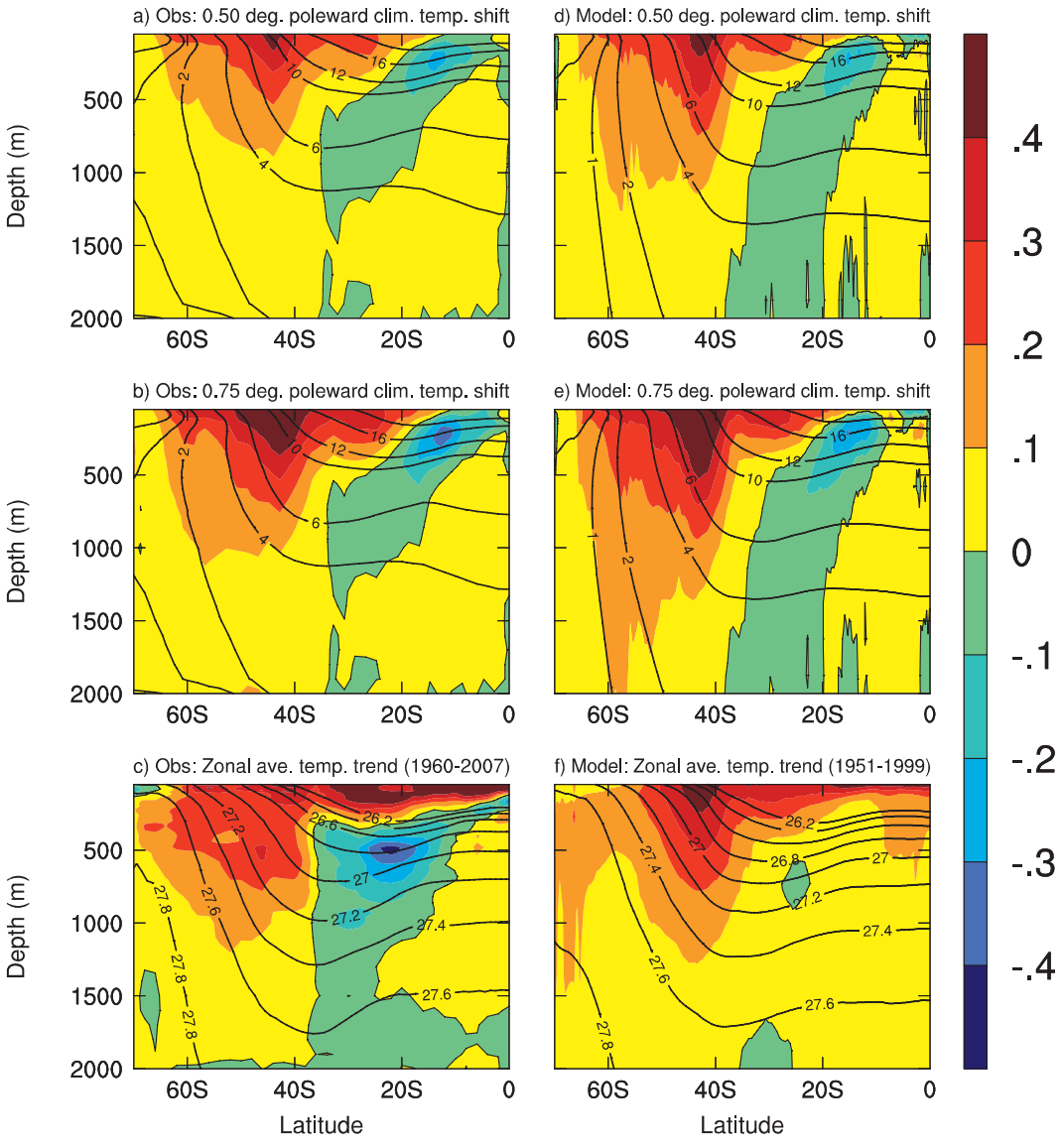

FIG. 4. (a),(b) Zonal-mean temperature changes (°C) resulting from (a) 0.5° and (b) 0.75° poleward shifts in the observed climatology, and (c) total trends in the observed (°C per 48 years) over the 1960–2007 period based on observations after correcting for instrumental errors (Wijffels et al. 2008). In (a) and (b) the climatological isotherm (°C) and in (c) the isopycnal (kg m^{-3}, from the Levitus climatological mean) contours are shown. (d)–(f) As in (a)–(c) but from the all-model ensemble mean (based on the 1951–99 period).

discussed previously. To further test this hypothesis, we take the corrected climatological temperature field (Wijffels et al. 2008) and shift the latitudes poleward by 0.5° and 0.75°, respectively, to form two shifted fields. The difference between the shifted and the original field reflects what such shifts would do in altering ocean temperatures. They are shown in Figs. 4a and 4b, to be compared with observed trends based on Wijffels et al. (2008), as shown in Fig. 4c. For a comparison, we perform a similar manipulation on the all-model ensemble mean climatology, with the results plotted in Figs. 4d–f.

The pattern after such a shift (Fig. 4a for a 0.5° shift case and Fig. 4b for a 0.75° shift) is indeed similar to the actual warming pattern (Fig. 4c), including a fast warming rate in the 35°–50°S midlatitude band, a hint of cooling to the north, and a top-to-bottom warming pattern centered at approximately 43°S. Sensitivities to the amount of the poleward shift—for example, by 0.75° and 1.5° (not shown)—reveal that the maximum warming always occurs at approximately 43°S, where the meridional temperature gradient in the climatology is a maximum, and that the amplitude of warming increases with

TABLE 1. Latitudinal band changes in the all-model oceanic heat content and the required equivalent surface heat flux change over a 49-year period (1951–99), based on poleward shifts of 0.5° and 0.75°. The surface heat flux change is calculated using the first equation, shown in section 2.

	Oceanic heat content change ($\times 10^{22}$ J)		Equivalent surface heat flux changes ($\overline{F_{\text{surf}}}$, W m^{-2})	
Latitude band	0.5° shift	0.75° shift	0.5° shift	0.75° shift
90°S–0°	7.95	11.0	0.205	0.283
50°–35°S	4.53	6.26	0.597	0.825
35°S–0°	0.354	0.482	0.016	0.021

the extent of the shift. The warming structure, with maximum warming located in the 35°–50°S midlatitude band as a result of a poleward shift, is consistent with that obtained from the Godfrey model (Fig. 3), which further highlights the central role of the wind changes in determining the latitudinal structure. The case of the 0.5° latitude shift, although it produces smaller subsurface temperature changes, matches well with the actual surface warming, particularly in the 35°–50°S midlatitude band; whereas, the 0.75° shift case produces a latitudinal band surface warming that is far too strong. These features are true of the all-model ensemble mean results. Compared with the observed, the modeled climatological mean temperature and isopycnals (Fig. 4, contours) are reasonably simulated, giving rise to the strong similarity between Figs. 4a and 4d and between Figs. 4b and 4e. Further, the structure of the observed and modeled trends is rather similar, although the modeled subsurface cooling is far weaker.

A significant difference between the observed and modeled trends is that the model climatological ocean is warmer, and model isotherms are more diffused and therefore deeper/steeper (e.g., 4°/2°C isotherms). These biases might be partly compensated by salinity, as indicated by the reasonably simulated density climatology (Fig. 4c, contours) when compared with the Levitus long-term mean (Levitus et al. 2000) (Fig. 4f, contours). However, a consequence of the more-diffused isotherms is that less heat stays at the near-surface depths, and more heat is transferred to the deep ocean. This may partly contribute to the small subsurface cooling. Other factors include an underestimated cooling as a result of volcanic forcing not being represented by all models or the indirect effect of anthropogenic aerosols not being fully incorporated into some models, in addition to the overly diffusive isotherms.

Although a poleward shift provides a convenient explanation of the pattern of warming, such a shift does not imply an ''adiabatic'' redistribution of heat. In effect, this shift indicates an expansion of the volume of warm water. Table 1 lists changes in oceanic heat content, the volume-averaged temperature changes, and the equivalent surface heat flux based on 0.5° and 0.75° shifts, respectively. With respect to the smaller shift of 0.5°, there is an increase in the oceanic heat content of 7.95×10^{22} J over the SH ocean. This is equivalent to a 0.21 W m^{-2} increase in net surface heat flux averaged over the SH ocean surface for the 49-year period. A larger poleward shift of 0.75° increases the heat content to 11.0×10^{22} J (equivalent to 0.28 W m^{-2}). Although these values are smaller than the actual all-model average change in surface heat flux of 0.50 W m^{-2}, they do imply a substantial heat gain by the SH oceans to support the shift. Such a heat gain can only be derived from either SH surface heat fluxes and/or a heat transfer from the NH across the equator. The latter is not possible, because the all-model average heat flux change over the NH is smaller than that needed for an increase in the NH ocean heat content. This is a feature consistent with a cross-hemispheric heat transport from the SH oceans to the NH oceans in response to an aerosol-induced cooling, which is greater in the NH (Cai et al. 2006). North of 35°S to the equator, the heat content change in the shifted field is negligible, with equivalent surface heat fluxes almost 40 times smaller than those in the 35°–50°S midlatitude band. Thus, averaged over the SH the majority of the greenhouse-induced heat gain goes to support this poleward shift in the circulation.

The aforementioned exercise supports the notion that to account for the top-to-bottom warming feature, a poleward shift is a most likely scenario, but such a shift is not adiabatic and involves heat input to the ocean. Next, we show that the fast warming rate in the 35°–50°S midlatitude band in the CMIP3 models, which do not resolve oceanic eddies, is driven not by local surface heat flux changes but by a strong heat gain south of 50°S.

5. Surface heat flux trends

The generation of changes in the various heat flux components is in itself rather revealing. As in the previous sections, surface heat flux changes averaged over 17 models are presented. In all heat flux components, a positive value means a heat gain by the ocean. An increasing mean sea level pressure, north of approximately 45°S and in association with an upward trend of

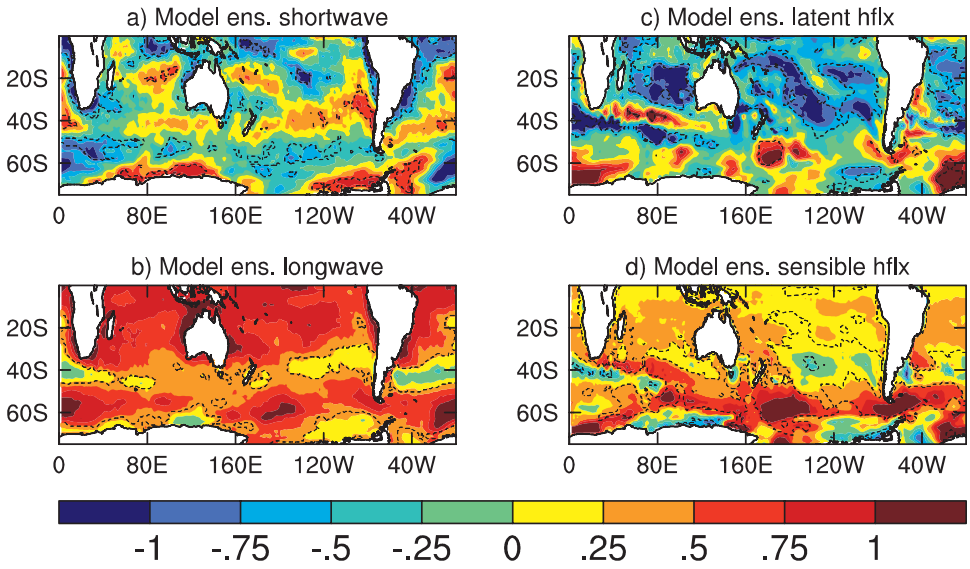

FIG. 5. All-model ensemble-mean changes in heat flux components (W m^{-2}) averaged over 1951–99: (a) net shortwave, (b) net longwave, (c) latent, and (d) sensible. All components are adjusted so that a positive value means that the ocean gains heat. Significant trends at the 95% confidence level are shown as areas within the dashed lines.

the SAM, leads to an increase in the net shortwave flux into the ocean. In the south the opposite is true, with a reduction (Fig. 5a) extending to about 60°S in association with an increased cloud cover as a consequence of the poleward shift of storm tracks (Yin 2005). The net longwave flux is positive everywhere (a greenhouse-warming signature), with a minimum around 40°S, where cloudiness decreases, but with a maximum south of 50°S (Fig. 5b) where cloudiness increases. Although increased westerlies in the 50°–60°S latitude band have an effect of enhancing evaporation, the decreased shortwave radiation and the associated weak surface cooling tend to offset it; therefore, the net effect is a small change in this component (Fig. 5c). The largest contribution to an increase in heat fluxes south of 50°S is from sensible heat fluxes resulting from an atmosphere warming faster (Fig. 5d) than the ocean, which is associated with the well-known polar amplification of warming, as sea ice and snow retreat (Manabe and Stouffer 1980). Thus, south of 50°S, despite the decrease in shortwave radiation, sensible and longwave flux changes add to a positive heat flux, resulting in a strong net heat gain to the ocean (Fig. 6, color) that is far larger than that over the 35°–50°S midlatitude band. Averaged globally and over the SH, the heat flux changes are 0.50 ± 0.15 and 0.53 ± 0.20 W m^{-2}, respectively. The uncertainty range is calculated as the standard deviation value of the intermodel variations.

The latitude band with the largest surface heat flux change does not coincide with the band with the fastest ocean warming, as can be seen from comparison of Fig. 2c and Fig. 6. Averaged over the 35°–50°S band, the surface heat flux change is 0.31 W m^{-2} and the implied oceanic heat content is small at 2.28×10^{22} J (Fig. 6, orange circle with cross) with a large standard deviation of intermodel variations. The heat flux change is far smaller than that required by a 0.5° or 0.75° poleward shift (Table 1) or the actual oceanic heat content increases of $6.46 \pm 3.31 \times 10^{22}$ J. Thus, on average, the implied heat content trend from the heat flux change accounts for only 35% of the warming within this band. The remaining 65% must be derived from outside the 35°–50°S band through meridional heat transfer (the sum of advection and diffusion).

Averaged over the high-latitude band from 50°S to the Antarctic coast, the heat flux change is 1.22 W m^{-2} and the implied oceanic heat content increase is 8.70×10^{22} J (Fig. 6, light blue circled cross), with a strong intermodel consensus. The implied heat content increase exceeds what is required for the actual heat content increase of $4.43 \pm 2.28 \times 10^{22}$ J from 50°S to the Antarctic coast. Heat transfer from the high latitude into the midlatitude band across 50°S is computed as the difference between the implied and the actual heat content increase, giving a northward heat transfer of 4.27×10^{22} J (Fig. 6, red arrow). Similarly, a transfer across 35°S of 0.087×10^{22} J (Fig. 6, orange arrow) is derived, which is computed as the difference between the sum of incoming heat transfer from 50°S and the heat gain from the atmosphere minus the heat required for the actual heat content increase over

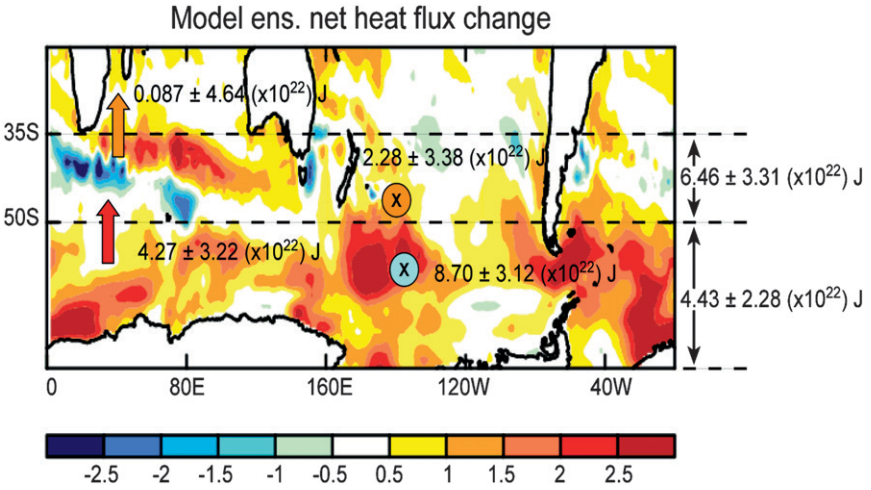

FIG. 6. All-model ensemble-mean net heat flux changes for 1951–99 (color contour; W m^{-2}) and the implied heat content increase over several latitude bands. The area confined by the two dotted lines along 50° and 35°S indicates where maximum warming occurs. The light blue ''circle cross'' indicates the equivalent heat content change over the area 50°S poleward from the heat flux change in this band (1.22 ± 0.44 W m^{-2}). The standard deviation of intermodel variations is indicated after the mean value. The north-pointing red arrow across 50°S denotes northward heat transfer, calculated as the difference between the equivalent heat content change from the heat flux and actual heat content change over the area 50°S poleward. The orange ''circle cross'' denotes the equivalent heat content change from the heat flux change over the 35°–50°S midlatitude band (0.31 ± 0.45 W m^{-2}). The north-pointing orange arrow across 35°S denotes heat transfer, calculated as the difference between incoming heat and that required for the warming in the 35°–50°S midlatitude band.

the midlatitude band. Overall, almost 50% of the surface heat gain south of 50°S is transferred northward and there is little heat transfer across 35°S.

What is the process responsible for taking surface heat gain south of 50°S to the 35°–50°S midlatitude band? As discussed by many previous studies (Bindoff and Church 1992; Johnson and Orsi 1997; Wong et al. 1999), isopycnals in the ACC latitudes tilt steeply from a deep depth to outcrop at the surface, as seen in Figs. 4c and 4f. Surface Ekman transport, enhanced by poleward-intensifying winds, carries upwelled water northward, where it gains heat from the atmosphere before it sinks along isopycnals again to form Antarctic Intermediate Water or Mode Water. The heat penetrates the ocean along isopycnal surfaces, and the surface heat fluxes outside the latitude band contribute to warming at a great depth within the band.

Is the process simulated by models? The zonally averaged density structure, averaged over these models (Fig. 4f), shows that isopycnals that outcrop across 50°–60°S, where the heat flux trend is the greatest, are those between $\sigma = 27.4$ and $\sigma = 26.4$. At 43°S, the $\sigma = 26.4$ line tilts downward to about 300 m, but $\sigma = 27.4$ extends downward to a depth of over 1000 m, allowing the surface heat to warm the ocean's upper 1000 m. The structure of the model isopyncals resembles that of the observed (Fig. 4c). There is no evidence that a latitude shift in the order of 0.5° will materially change the process, the depth of heat penetration, or the efficiency of the process.

Thus, the very weak change in heat content in the ensemble of models north of 35°S and below 500 m, as seen in Fig. 4f, occurs because in the model the wind-forced rate of change of heat content in the 35°–50°S midlatitude band takes up nearly all the extra heat transported from south of 50°S. In reality, the ratio of the southern heat flux to the wind-forced rate of change of heat content in 35°–50°S is less than in the models, so some heat has to be supplied from the north, cooling the 35°–15°S subsurface region.

In summary, the subsurface cooling north of the 35°–50°S midlatitude band and the significant warming below ventilation within this band both indicate the importance of a wind-driven poleward shift. However, such a shift requires an increase in heat input to the SH ocean in all latitude bands (Table 1), with the largest in the 35°–50°S midlatitude band. The majority of the heat comes from south of 50°S. In other words, a poleward shift can only occur in the presence of a heat flux input to the SH ocean. Counterintuitively, much of the heat gain required is provided from the south, and the picture that emerges is that a wind-induced poleward shift and the

associated increase in northward Ekman transport, a polar amplification of warming, and heat penetration along the isopycnal surfaces all contribute to the fast, top-to-bottom warming in the 35°–50°S midlatitude band.

Recent studies have shown that models that do not resolve eddies may have overestimated the role of northward Ekman transport. In eddy-resolving models, the impact of Ekman transport will be offset by eddy fluxes, which increase in response to the stronger westerly winds (Meredith and Hogg 2006; Fyfe et al. 2007). Supporting evidence for this feature is that the isopycnal tilts across the ACC have not changed much over the past decades (Böning et al. 2008), which is consistent with the significant role of eddy fluxes in compensating the enhanced Ekman transport. Thus, in eddy-resolving models a far larger portion of heat needed to warm the 35°–50°S midlatitude band may come from local surface fluxes, rather than from fluxes south of 50°S. This means that the composition and/or magnitude of the heat flux trends south of 50°S would be rather different from what we have described. There are already suggestions that the modeled response to global warming in terms of the Southern Ocean energy budget is rather unrealistic (Trenberth and Fasullo 2010). The relative importance of mesoscale eddies and Ekman transport in the overall heat and momentum balance of the Southern Ocean response is a topic of great interest (Fyfe et al. 2007; Spence et al. 2009, manuscript submitted to *J. Climate*; Spence et al. 2009).

6. Conclusions

We explore the drivers of the fast, deep ocean warming in the 35°–50°S midlatitude band, in particular, the relative importance of forcing from changes in the wind and surface heat fluxes. Using wind and heat flux outputs from 17 CMIP3 twentieth-century experiments, we show that the fast, deep warming is unable to be accounted for by the direct heat flux changes over the midlatitude band, which is consistent with the finding of a nonlocal balance (e.g., Pierce et al. 2006). The vertical structure and zonal distribution of the warming in this midlatitude band are consistent with a Sverdrup-type response to changes in winds and with both a poleward shift of the SH supergyre and the ACC of less than 1° latitude, consistent with results from previous studies (Cai et al. 2005; Cai 2006; Alory et al. 2007; Gille 2008). An important advance is that such a poleward shift is not adiabatic and involves an oceanic heat content increase, with a maximum in this latitude band, which can only result from an increase in surface heat fluxes into ocean. Counterintuitively, the net heat required for warming in this midlatitude band is largely derived from surface heat fluxes south of 50°S, where the changes are an order of magnitude greater than that over the 35°–50°S midlatitude band, associated with a polar-amplification of warming. Our result highlights the symbiosis of the wind and surface heat flux response. However, none of the models resolve eddies; given that eddy fluxes could offset the increase in the northward Ekman transport, the heat source for the fast, deep warming in the midlatitude band could be rather different from that in the real world. In eddy-resolving models, a far larger portion of heat needed to warm the midlatitude band may come from local surface fluxes. This means that the response of the Southern Ocean in the real world could be rather different from what is simulated. Therefore, the difference represents a significant source of uncertainty in future climate projections using these models.

Acknowledgments. W. Cai, T. Cowan, and S. Wijffels are supported by the Australian Department of Climate Change. We thank the many modeling groups and institutions for the use of their climate model output and recognize the significant work that the Program for Climate Model Diagnosis and Intercomparison (PCMDI) has undertaken in collecting and storing the model data. For more details on model data or documentation, readers are referred to the PCMDI Website (available online at http://www-pcmdi.llnl.gov).

REFERENCES

Alory, G., S. Wijffels, and G. Meyers, 2007: Observed temperature trends in the Indian Ocean over 1960–1999 and associated mechanisms. *Geophys. Res. Lett.,* **34,** L02606, doi:10.1029/2006GL028044.

Arblaster, J. M., and G. A. Meehl, 2006: Contributions of external forcings to southern annular mode trends. *J. Climate,* **19,** 2896–2905.

Banks, H., and R. Wood, 2002: Where to look for anthropogenic climate change in the ocean. *J. Climate,* **15,** 879–891.

Barnett, T. P., D. W. Pierce, K. M. AchutaRao, P. J. Gleckler, B. D. Santer, J. M. Gregory, and W. M. Washington, 2005: Penetration of human-induced warming into the world's oceans. *Science,* **309,** 284–287.

Bindoff, N. L., and J. A. Church, 1992: Warming of the water column in the southwest Pacific Ocean. *Nature,* **357,** 59–62.

Böning, C. W., A. Dispert, M. Visbeck, S. R. Rintoul, and F. U. Schwarzkopf, 2008: The response of the Antarctic Circumpolar Current to recent climate change. *Nature Geosci.,* **1,** 864–869, doi:10.1038/ngeo362.

Cai, W., 2006: Antarctic ozone depletion causes an intensification of the Southern Ocean super-gyre circulation. *Geophys. Res. Lett.,* **33,** L03712, doi:10.1029/2005GL024911.

——, and T. Cowan, 2007a: Impacts of increasing anthropogenic aerosols on the atmospheric circulation trends of the Southern Hemisphere: An air–sea positive feedback. *Geophys. Res. Lett.,* **34,** L23709, doi:10.1029/2007GL031706.

——, and ——, 2007b: Trends in Southern Hemisphere circulation in IPCC AR4 models over 1950–1999: Ozone depletion vs. greenhouse forcing. *J. Climate,* **20,** 681–693.

——, P. H. Whetton, and D. J. Karoly, 2003: The response of the Antarctic Oscillation to increasing and stabilized atmospheric CO_2. *J. Climate,* **16,** 1525–1538.

——, G. Shi, T. Cowan, D. Bi, and J. Ribbe, 2005: The response of the southern annular mode, the east Australian Current, and the southern midlatitude ocean circulation to global warming. *Geophys. Res. Lett.,* **32,** L23706, doi:10.1029/2005GL024701.

——, D. Bi, J. Church, T. Cowan, M. Dix, and L. Rotstayn, 2006: Pan-oceanic response to increasing anthropogenic aerosols: Impacts on the Southern Hemisphere oceanic circulation. *Geophys. Res. Lett.,* **33,** L21707, doi:10.1029/2006GL027513.

Church, J. A., N. J. White, and J. M. Arblaster, 2005: Significant decadal-scale impact of volcanic eruptions on sea level and ocean heat content. *Nature,* **438,** 74–77.

Delworth, T. L., V. Ramaswamy, and G. L. Stenchikov, 2005: The impact of aerosols on simulated ocean temperature and heat content in the 20th century. *Geophys. Res. Lett.,* **32,** L24709, doi:10.1029/2005GL024457.

Fyfe, J. C., 2006: Southern Ocean warming due to human influence. *Geophys. Res. Lett.,* **33,** L19701, doi:10.1029/2006GL027247.

——, G. J. Boer, and G. M. Flato, 1999: The Arctic and Antarctic Oscillations and their projected changes under global warming. *Geophys. Res. Lett.,* **26,** 1601–1604.

——, O. A. Saenko, K. Zickfeld, M. Eby, and A. J. Weaver, 2007: The role of poleward-intensifying winds on Southern Ocean warming. *J. Climate,* **20,** 5391–5400.

Gille, S. T., 2002: Warming of the Southern Ocean since the 1950s. *Science,* **295,** 1275–1277.

——, 2008: Decadal-scale temperature trends in the Southern Hemisphere ocean. *J. Climate,* **21,** 4749–4765.

Godfrey, J. S. A., 1989: A Sverdrup model of the depth-integrated flow for the World Ocean allowing for island circulations. *Geophys. Astrophys. Fluid Dyn.,* **45,** 89–112.

Hansen, J., and Coauthors, 2005: Earth's energy imbalance: Confirmation and implications. *Science,* **308,** 1431–1435.

Johnson, G. C., and A. H. Orsi, 1997: Southwest Pacific Ocean water-mass changes between 1968/69 and 1990/91. *J. Climate,* **10,** 306–316.

Kushner, P. J., I. M. Held, and T. L. Delworth, 2001: Southern Hemisphere atmospheric circulation response to global warming. *J. Climate,* **14,** 2238–2249.

Levitus, S., J. Antonov, T. Boyer, and C. Stephens, 2000: Warming of the world ocean. *Science,* **287,** 2225–2229.

——, ——, and ——, 2005: Warming of the world ocean, 1955–2003. *Geophys. Res. Lett.,* **32,** L02604, doi:10.1029/2004GL021592.

Manabe, S., and R. J. Stouffer, 1980: Sensitivity of a global climate model to an increase of CO_2 concentration in the atmosphere. *J. Geophys. Res.,* **85,** 5529–5554.

Meehl, G. A., and Coauthors, 2007: Global climate projections. *Climate Change 2007: The Physical Science Basis,* S. Solomon et al., Eds., Cambridge University Press, 747–845.

Meredith, M. P., and A. M. Hogg, 2006: Circumpolar response of Southern Ocean eddy activity to a change in the southern annular mode. *Geophys. Res. Lett.,* **33,** L16608, doi:10.1029/2006GL026499.

Oke, P. R., and M. H. England, 2004: Oceanic response to changes in the latitude of the Southern Hemisphere subpolar westerly winds. *J. Climate,* **17,** 1040–1054.

Palmer, M. D., K. Haines, S. F. B. Tett, and T. J. Ansell, 2007: Isolating the signal of ocean global warming. *Geophys. Res. Lett.,* **34,** L23610, doi:10.1029/2007GL031712.

Pierce, D. W., T. P. Barnett, K. M. AchutaRao, P. J. Glecker, J. M. Gregory, and W. M. Washington, 2006: Anthropogenic warming of the oceans: Observations and model results. *J. Climate,* **19,** 1873–1900.

Ridgway, K. R., and J. R. Dunn, 2007: Observational evidence for a Southern Hemisphere oceanic supergyre. *Geophys. Res. Lett.,* **34,** L13612, doi:10.1029/2007GL030392.

Roemmich, D., and J. Gilson, 2009: The 2004–2008 mean and annual cycle of temperature, salinity, and steric height in the global ocean from the Argo program. *Prog. Oceanogr.,* **82,** 81–100, doi:10.1016/j.pocean.2009.03.004.

Spence, P., O. Saenko, M. Eby, and A. J. Weaver, 2009: The Southern Ocean overturning: Parameterized versus permitted eddies. *J. Phys. Oceanogr.,* **39,** 1634–1651.

Suzuki, T., and Coauthors, 2005: Projection of future sea level and its variability in a high-resolution climate model: Ocean processes and Greenland and Antarctic ice-melt contributions. *Geophys. Res. Lett.,* **32,** L19706, doi:10.1029/2005GL023677.

Thompson, D. W. J., and S. Solomon, 2002: Interpretation of recent Southern Hemisphere climate change. *Science,* **296,** 895–899.

Trenberth, K. E., and J. T. Fasullo, 2010: Simulation of present-day and twenty-first-century energy budgets of the southern oceans. *J. Climate,* in press.

Wijffels, S. E., J. Willis, C. M. Domingues, P. Barker, N. J. White, A. Gronell, K. Ridgway, and J. A. Church, 2008: Changing expendable bathythermograph fall rates and their impact on estimates of thermosteric sea level rise. *J. Climate,* **21,** 5657–5672.

Wong, A. P. S., N. L. Bindoff, and J. A. Church, 1999: Large-scale freshening of intermediate waters in the Pacific and Indian Oceans. *Nature,* **400,** 440–443.

Yin, J. H., 2005: A consistent poleward shift of the storm tracks in simulations of 21st century climate. *Geophys. Res. Lett.,* **32,** L18701, doi:10.1029/2005GL023684.